LA-6997-MS
Informal Report

UC-34
Issued: November 1977

Exploratory Laser-Driven Shock Wave Studies

J. C. Solem
L. R. Veeser

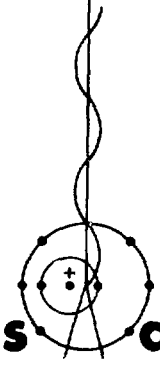

los alamos
scientific laboratory
of the University of California
LOS ALAMOS, NEW MEXICO 87545

UNITED STATES
DEPARTMENT OF ENERGY
CONTRACT W-7405-ENG. 36

EXPLORATORY LASER-DRIVEN SHOCK WAVE STUDIES

by

J. C. Solem and L. R. Veeser

ABSTRACT

We show the results of a feasibility study for investigating shock structure and for measuring equation-of-state parameters using high-energy, short-pulse lasers. We discuss the temporal and spatial structure of the luminosity from laser-driven shock unloading in aluminum foils. We demonstrate that shock velocity can be measured by observing the time interval between shock emergence across two thicknesses and show data for shocks of 1.3 and 2.1 Mbar. The fact that we observe shock fronts cleanly breaking through steps as small as 3 μm indicates that the shock front thickness is very small in the few megabar region; this is the first experimental verification that these fronts are not more than a few micrometers thick. We present approximate measurements of free-surface velocity. Finally, we speculate on the use of these techniques to obtain detailed equation-of-state data.

I. INTRODUCTION

Part of the justification for the laser fusion program at its inception was that it might contribute to our understanding of nuclear weapons physics. This was a well-founded justification because the power densities realized at the focus of high-energy, short-pulse lasers are matched only in nuclear explosions. These power densities are achieved by no other laboratory device. Although the present level of laser technology is not such that it can be done easily, there is no other laboratory means of studying such high-power density physics.

One area of physics of particular interest to weapons designers is hydrodynamics at high-energy density, and a particular subset is the structure of shock waves and high-pressure equations-of-state (EOS). Shock waves can be studied and EOS parameters can be measured in actual nuclear tests, but this is expensive and the number of available experiments is very limited. It is also difficult to look at the microscopic structure of shocks on nuclear tests.

We have been exploring the use of high-energy lasers to study shock structure and measure EOS parameters. Work of this type has been undertaken by several researchers[1-3] using thick, transparent targets. They observed shock waves traveling through the materials by shining a second laser through a sample onto a camera, and they deduced pressures, densities, and temperatures behind the shock.

Because we would like to look at thin, opaque samples, sidelighting with another laser will not work. However, we believe that we can measure shock velocity and perhaps free-surface velocity for such a sample. Shock velocity can be measured by a technique analogous to that used on nuclear tests. In Nevada we set light pipes at various depths into materials and observe the shock arrival at these depths by the emerging shock's own luminosity, which is usually recorded by an array of photomultipliers.[4,5] In the case of a laser-driven shock, we can use an ultrahigh-speed streak camera to time the shock arrival by observing the light emitted from various layers (see Fig. 1).

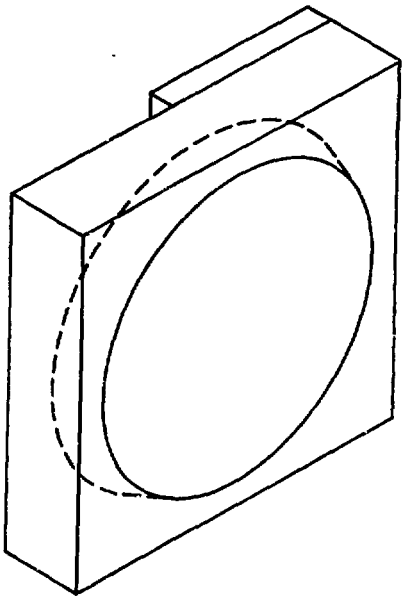

Fig. 1. Schematic of target used in measuring shock velocities. Energy from the laser pulse is deposited near the surface of the target (solid circle) and generates hot electrons, which redeposit the energy in the volume nearby (dashed region). The sudden heating of the target sets up a shock wave that traverses the foil and emerges first from the substrate and later from the thin layer covering half of the back of the target. The thickness of the thin layer divided by the difference in emergence times is the shock velocity.

Because the shock front sets up somewhere inside the foil, the time delay between the laser pulse striking the foil and the emergence of the shock front does not give the shock velocity. However, by making the foil have two or more thicknesses (by evaporating at least one extra layer onto the back), we can determine the shock velocity from the difference in emergence times from the layers if we know the difference in thickness. Free-surface velocity can be measured by simply observing the motion of the back surface with a streak camera. This assumes that the depth of the radiating layer is reasonably constant and two-dimensional effects are negligible.

One difficulty that we have with laser-driven shocks, but do not have in nuclear tests, is the presence of a large quantity of superthermal electrons. In thin foils these electrons will preheat the test material before a shock is driven through it. Experiments to determine the spectrum of these electrons for 1.06-μm-wavelength light show that about 90% of their energy is redeposited every 8 μm.[6] More detailed theoretical examination of this problem shows the spectrum to be a function of intensity as well,[7,8] but the 8-μm figure is a good estimate for our range of intensities. The thicker we make the foil into which we are depositing the laser energy, the less preheating we will get at the back. On the other hand, the thicker the foil, the more likely it is that a rarefaction will overtake the shock before it breaks through the back surface. Thus we have definite upper and lower bounds on target thickness for a given laser energy, pulse length, and wavelength. Furthermore, since the laser spot size must be large compared with the foil thickness if we are to maintain a semiplanar shock, we are limited in the pressure we can obtain for a given laser. In general we feel that the foil must be more than 8 μm thick and the laser spot more than 100 μm for a meaningful measurement.

The studies in this report are to be considered a precursor to more in-depth work in both EOS and shock structure. This has been a feasibility study to assess the state of the art in instrumentation and lasers to see how well they can address this sort of problem.

II. APPARATUS

A. Laser

The high-energy, short-pulse laser for all the experiments reported here was the four-beam, 1.06-μm neodymium-glass laser built by L Division in Bldg. 46 of Ten Site.[9,10] The system consists of a mode-locked oscillator, three YAG amplifiers, three rod amplifiers, and four sets of sixteen 86-mm disk amplifiers, one set for each beam. We used only one beam.

A single beam line is capable of delivering about 100 joules for a 1-ns-long pulse, but we used pulses in the range from 10 to 50 joules. The system includes calorimeters for measuring the total beam output as well as energy at various stages. The energies we record for individual shots

are accurate to within 10% with a relative error of about 3%. The laser energy is not reproducible from shot to shot; energies can be recorded but not predicted.

Our nominal pulse length was 300-ps FWHM, with an approximate Gaussian shape in time. Most of our data were recorded with this kind of pulse. Occasionally the laser would produce a double pulse with peak spacing of about 2 ns. This results from malfunctioning of the oscillator, whose normal pulse-train spacing is 10 ns (long compared with the time scale of events we are trying to observe). We assume that the first half of such a double pulse tended to extract most of the energy from the amplifiers. We noticed no significant difference between double-pulse data and single-pulse data except when the first pulse was too small to trigger the streak camera. We tried some experiments with 1-ns pulses in an attempt to realize more energy per pulse, but we abandoned the effort because the laser would not perform reliably at that pulse length.

The beam spot at the target could be easily varied from a roughly circular disk about 50 μm in diameter to a roughly elliptical shape about 200 μm by 400 μm. The intensity distribution of the minimum diameter is purported to be nearly Gaussian; presumably the larger focal spots are more uniform. The elliptical pattern can be oriented either vertically or horizontally, depending on whether the focal point was placed in front of or in back of the target. The spot could be defocused to larger sizes, but we avoided using larger diameters because the reduced intensities made shocks that were too weak to record. Spot dimensions were measured to within about ± 20%.

B. Optical System

Figure 2 shows the layout of our optical system for imaging the emerging shock waves and expanding plasma on the slits of the streak camera. The main reason for viewing the foils from a 45° angle rather than normal to the target was to avoid propagating the laser pulse down the optics and damaging the camera photocathode. We further protected the camera by putting filters in front of the slits. The 45° angle also allowed us to estimate the velocity of the blow-off material after shock penetration.

The f/1.18, 55-mm achromatically corrected objective lens provided the greatest light-gathering capability available for an off-the-shelf system. The chromatic aberration of the system was negligible for our purposes. The objective lens could either be used to project parallel rays to a similarly corrected f/4.5, 304-mm lens mounted on the camera for a magnification of 5.5, or the objective lens could be focused directly on the slits for a magnification of about 33. The greater magnification reduced intensity at the slits. Generally, we used slit widths of about 0.5 mm.

In early experiments we used simple lenses in a configuration similar to Fig. 2 with a mirror in front of the objective lens to bring the image out at 90° to the beam.

C. Streak Cameras

Figure 3 shows a schematic of the type of streak camera used.[11] Light from the optical system passed through the image slit and a lens inside the camera before striking the photocathode. The emerging electron beam was accelerated and focused through an aperture in the anode. The beam passed between two deflecting plates and struck a fluorescent screen where an image was formed. A rapidly varying voltage was applied to the plates to deflect the beam, making a streak the width of

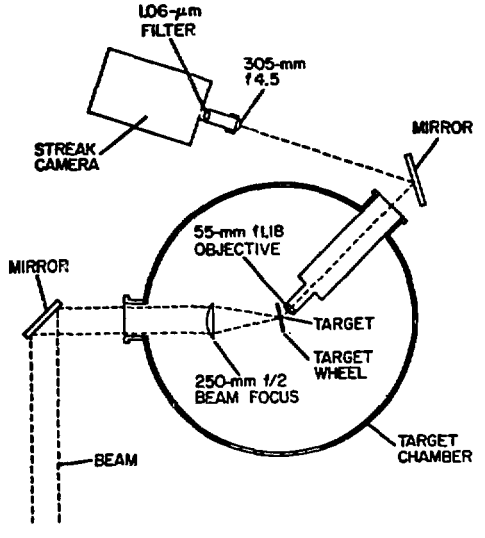

Fig. 2. Optical arrangement in the target room.

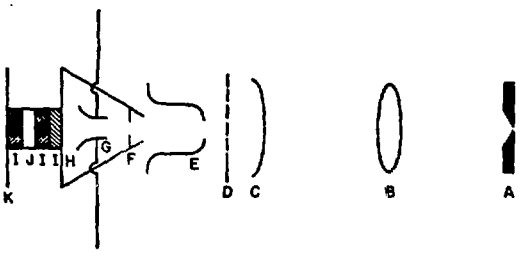

Fig. 3. Schematic of the streak camera: A) object slits; B) internal lens; C) photocathode; D) grid; E) focus electrode; F) anode; G) deflection plates; H) fluorescent screen; I) fiberoptical couplers; J) image intensifier; K) film. Elements C through H are contained in the image tube.

the slit. An intensifier was used between the screen and the film to increase the camera sensitivity. To further maximize the sensitivity, and hence the speed of the camera, it was run with the largest possible electron beam current passing through the aperture when there was enough light on the slit to make a useful image. Unfortunately, this condition tends to limit the dynamic range, but because we needed to collect as much light as possible, we did not feel we could reduce the sensitivity.

In our first experiments we used an RCA-image-tube-based, S-1 photocathode streak camera designed and built by Dean Sutphin (Group J-14). At that time we believed, on the basis of calculations, that most of the light from the emerging shock would be in the infrared, with a roughly Planckian distribution peaking around 1 eV. It turned out that with temperatures this low, the total intensity was insufficient to image the shock-wave emergence. When we reduced the laser spot size enough to see the shock, and consequently increased the postshock temperature, we found that most of the emitted light was in the visible. We established this fact by focusing an uncorrected lens system first in the infrared and then in the visible, and then comparing the resolution of the streaks.

Because the sensitivity limitation of the S-1 photocathode forced us to increase the shock strength until the observed radiation was in the visible, it obviated the original advantage of the S-1, namely its sensitivity to infrared light. We decided to use an S-20 camera instead. The S-20 is nearly two orders of magnitude more sensitive in the visible.

The first S-20 camera was nearly identical to the S-1 camera. Although it was useful, it suffered from several disadvantages: 1) it had only one streak speed (~ 80 ps/mm); 2) it had a low sensitivity; and 3) it had a very limited dynamic range, owing at least in part to the age and condition of the image tube. We measured the dynamic range independently with a small ruby laser and found that it would cover intensity excursions of about a factor of three from overexposure to no image. Using a joule meter and beam splitter with the same ruby laser, we also measured the overall sensitivity. The threshold seemed to be about 300 watts/cm^2 on the slits. This is higher than expected for such an image tube and intensifier combination.

The most severe limitation was the dynamic range since a variation of 30% in brightness temperature could cause the image to go from gross overexposure to no exposure at all. We also needed to cover a larger time span, so a variable streak speed was desirable. The only camera available at the time that satisfied these requirements was an Electrophotonics ICC-512. Our most interesting data were acquired with this camera.

All three cameras were triggered by a pulse extracted from the oscillator and sent to a small silicon photodiode. For the RCA cameras we used an ORTEC-463 constant fraction discriminator to maintain the same relative trigger time over about a factor of two variation in height of the switched-out pulse. We checked the jitter in the triggering system by putting a photodiode in the beam and recording its pulse on an oscilloscope triggered by the pulse normally used as the input to the streak-camera gate. By superimposing many such pulses, we found a total jitter at the camera input of less than 100 ps. For the Electrophotonics camera, we triggered with a level discriminator having two or three times as much jitter.

All three cameras, however, seem to have had internal jitters or spontaneous drifts of several nanoseconds. This has been the single most frustrating aspect of the experiment. Many laser

pulses were wasted because the streak had moved off the field of view. It is clear that if serious EOS data are to be obtained in a reliable and routine manner, this type of triggering technology cannot be used. Perhaps a Mylar spark-gap trigger, when it becomes available, will provide a solution to this problem.

III. CHARACTER OF SHOCK PENETRATION

A. Luminosity at Shock Unloading

Figures 4a, b, c, and d are streaks of the light emerging from the backsides of 13-μm aluminum foils irradiated in nearly circular spots about 100 μm in diameter. The laser energies for the images are: a) 32 J; b) 37 J; c) 37 J; and d) 35 J. The streaks were recorded at different speeds from 0.1 to 1.0 ns/mm of film and all are at a magnification of 5.5. The streaks show an intense pulse of light about 800 ps in duration followed by dim light that persists for at least 25 ns. Figure 4d is purposely overexposed to show the dim trailing light. The exaggerated width at the start of the streak is a result of this overexposure.

We ascribe the intense light to the emergence of the shock wave and the trailing dim light to the plasma moving away from the surface. This interpretation is obscured if the distribution of hot electrons is significantly different from what is anticipated. The drop in intensity is likely a composite of cooling of the metal owing to radiative losses, obscuration by cooler plasma expanding at the surface, and the arrival of a rarefaction from the front. A simple analysis[12] of the luminosity of metallic vapors in unloading gives a logarithmic decrease of the radiation brightness temperature with time; $T_{br} \propto (\ln t + \text{const})^{-1}$. Although we have not investigated the nonlinear response of the photocathode-intensifier-film system, it would be very difficult for this simple analysis to account for the time dependence of the luminosity we observe.

The problem of determining the depth into which one is seeing is serious only after the shock has arrived. Before that time, the unheated aluminum should act as a good shield of light emitted by the shock traversing the foil, and the time when the shock reaches the surface should be well resolved. The horizontal lines seen in Figs. 4a and 4d are ascribed to scattered light impinging the slits. This is most likely either second harmonic laser light or Planckian radiation from the plasma blowoff on the laser side of the foil; essentially all 1.06-μm light is filtered out and the camera is not sensitive to infrared. Figure 4a shows that the expanding plasma spreads to a width of about 800 μm in 25 ns.

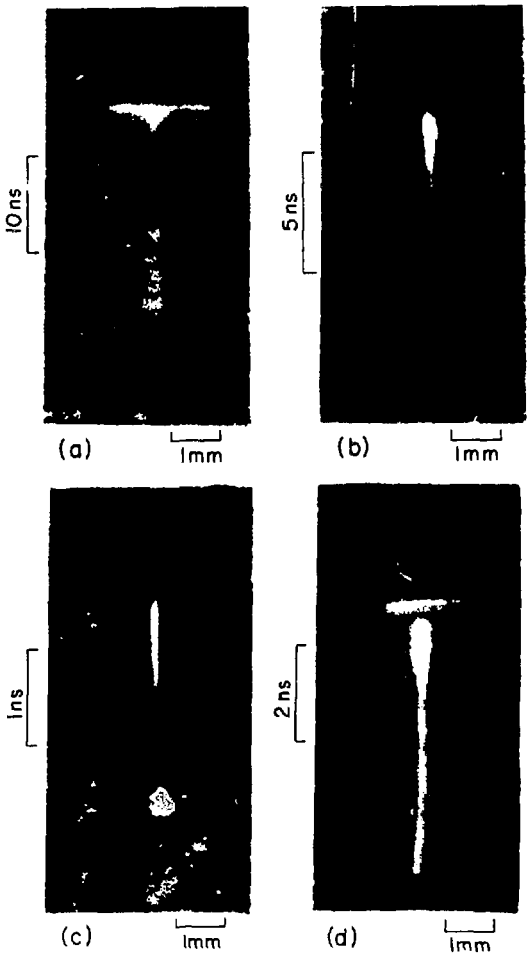

Fig. 4. Streak-camera data at low magnification (x 5.5) showing the time dependence of the light emerging from the backs of four 13-μm-thick aluminum targets after each was struck by a 100-μm-diam, 300-ps laser pulse of about 35 J. The streaks run from top to bottom. They show an intense light pulse that lasts for about 0.8 ns and is followed by a dimmer light lasting for at least 25 ns. Figure 4d is overexposed, exaggerating the initial bright pulse but clearly showing the first 6 ns of the tail.

Streaks similar to those in Fig. 4 were obtained for aluminum foils of 6, 18, and 25 μm. The intensity drops dramatically as the foil thickness is increased. Between 6 and 13 μm some of this drop could be attributed to the rapid attenuation of hot electrons, but between 13 and 25 μm this effect must result from decay of the shock wave. Whether the decay results from various energy-loss mechanisms or the overtaking of a rarefaction is undetermined and still under investigation.

B. Penetration Geometry

Figure 5 shows a typical penetration pattern at high magnification (x 33). The data shown are for a 33-J, 300-ps pulse in an elliptical spot about 50 μm by 150 μm on a 13-μm aluminum foil. (The major axis of the ellipse is aligned along the slits.) The somewhat jagged edge indicates a variation of 100 to 200 ps in breakthrough time for the shock front. This is well within the time-resolving power of the camera. While the jagged edge appears on all shots of this sort, it is generally smoother than the figure shown here. Typical variation is on the order of 50 ps.

The leading edge of the trapezoidal pattern is about 90 μm wide before magnification and the trailing section is about 180 μm wide. The laser-illuminated area was about 150 μm in the observed direction, so the semiplanar region is significantly smaller than the spot. One is first tempted to attribute this effect to lateral unloading[13] into the cold surrounding metal. The difficulty with this interpretation is that the width of the leading edge is too small. For example, if a 1.2-Mbar plane shock 150 μm in diameter were driven through a foil 13 μm thick, it would be expected to emerge with a plane region about 138 μm in diameter. What we see is much too small for the pressure range we expect. Therefore we ascribe the trapezoidal shape to a combination of lateral unloading and nonuniform laser-spot intensity distribution.

A particularly interesting feature of Fig. 5 is the small blob of intense light that appears on the right-hand side about 800 ps after the first shock breakthrough. This has to do with the 45° viewing angle and the way the blowoff tends to obscure the emerging shock (see Fig. 6). The exact details of this effect are not understood, but two theories may explain the data: 1) the free surface bulges out to a point where the edge near the objective lens is nearly normal to the line of sight and the radiating layer is viewed through a minimum optical depth; or 2) the laser blows a disk out of the foil (somewhat like a cookie cutter) and we see the hot plasma behind--consistent with the 800-ps delay. This feature, called the right-shoulder effect, is prominent and appears on nearly every shot.

C. Shock Velocity

We measure shock velocity by observing the time difference between shock emergence on the two sides of a measured step in the foil. Because the right-shoulder effect tends to obscure the breakthrough when the thick side is on the right, we

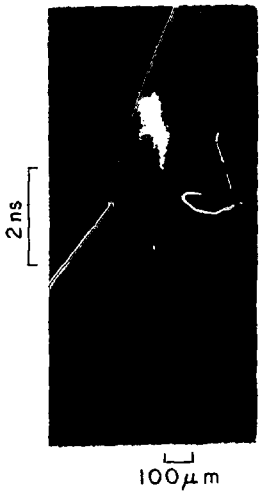

Fig. 5. Streak-camera data at high magnification (x 33). Time increases from top to bottom.

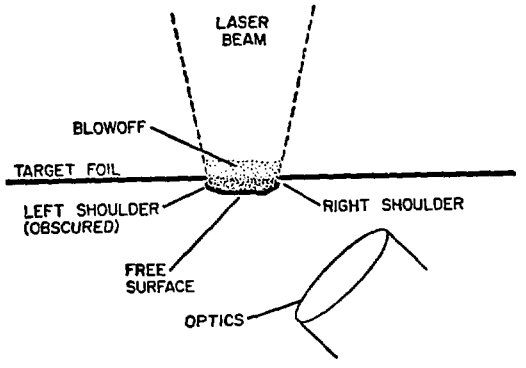

Fig. 6. Schematic of the target blowoff from the laser pulse showing how the left side of the plasma can be obscured by the moving free surface.

obtained unambiguous measurements of shock velocity only when the thick side was on the left.

Figure 7 shows a measurement of shock velocity in aluminum. The streak was obtained with the RCA-image-tube-based S-20 camera and is for a 300-μm by 400-μm elliptical focal spot with a 300-ps pulse of 37-J energy. The two sides of the step in the foil are 13 and 18 μm thick; the image of the thicker side is on the left. The streak is out of focus and overexposed, so it appears broader than it should. It shows the beginning of the right-shoulder effect in the lower right corner. The step on the left we ascribe to the shock breaking through the thick side. The time difference of about 450 ps corresponds to a velocity of about 1.1 cm/μs. The fact that the intensity is somewhat higher for the thin side of the step suggests again that the shock is decaying between 13 and 18 μm. The velocity corresponds to a pressure of about 1.3 Mbar.

Figure 8 shows a similar measurement with the Electrophotonics camera. Here the spot size is 250 μm by 100 μm and the 300-ps pulse had an energy of 26 J. We ascribe the step on the left to the shock breaking through the two thicknesses, which were 13 and 16 μm. The blob on the right, occurring somewhat later, is the right-shoulder effect.

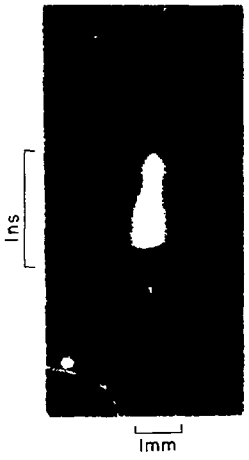

Fig. 7. Streak-camera data for a 13-μm-thick aluminum target with an additional 5-μm-thick layer of aluminum covering the left side of the spot struck by the laser. Time increases from top to bottom. The time delay of 450 ps for the shock to traverse the 5-μm layer indicates a pressure of about 1.3 Mbar behind the shock.

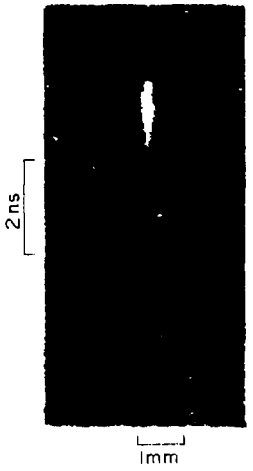

Fig. 8. Streak-camera data for a 13-μm-thick aluminum target with an additional 3-μm-thick layer of aluminum covering the left side of the spot struck by the laser. Time increases from top to bottom. The time delay of 230 ps for the shock to traverse the 3-μm layer indicates a pressure of about 2.1 Mbar behind the shock.

Measurement of the breakthrough time interval gives a shock velocity of 1.3 cm/μs, corresponding to a pressure of about 2.1 Mbar.

The purpose of the step experiments was to prove we could measure shock velocities by this technique with the intention of extending to impedance-matching experiments for obtaining EOS data. This was accomplished, but perhaps more importantly we have demonstrated that, at pressures of a few megabars, shock fronts are less than a few micrometers thick. This imposes constraints on the type of model one can use to describe viscosities in metals at these pressures.

D. Free-Surface Velocities

Since the heated back surface is visible for some time after the shock emerges, we can get some estimate of its velocity. Unfortunately, we do not know our exact depth of view into the expanding material. Furthermore, viewing from 45° can introduce some three-dimensional effects that also confuse data interpretation.

Figure 9 is an example of how the expanding plasma can be followed by the streak camera. This picture was taken with the Electrophotonics streak camera at a high-gain intensifier setting and x 33

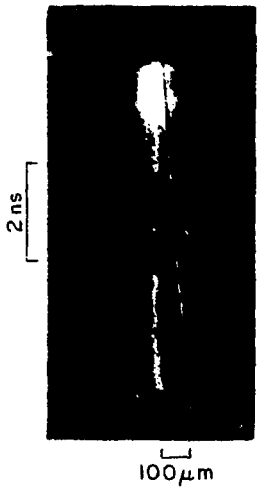

Fig. 9. Streak-camera data for a 13-μm-thick aluminum target. The dotted line shows the center of the camera slit. Time increases from top to bottom. The movement of the streak away from the marker indicates that the radiating plasma is moving about 1.3 cm/μs in the laser-beam direction.

magnification. The shock is driven by a 38-J, 300-ps pulse in an elliptical focal spot about 50 μm by 150 to 200 μm. The target is a plain 13-μm aluminum foil. The dotted line down the right side is a fiducial marker to give an accurate right-left motion measurement. The sweep does not follow a straight line, as can be seen by the nonlinearity of the marker. The movement of the plasma light is from right to left, which indicates motion of the surface away from the laser. The total movement shown on the streak is about 80 μm and the velocity is about 1.3 cm/μs. This intensity pulse would be expected to produce a shock velocity of about 1.4 cm/μs, so 1.3 cm/μs is a reasonable free-surface velocity.

Keeping in mind all the caveats associated with measuring a free-surface velocity by this method, it is at least encouraging to see numerical agreement between the shock velocity and what appears to be the velocity of the back of the foil. With adequate streak-camera dynamic range, there is no reason why we could not measure this motion and the shock velocity simultaneously.

IV. FUTURE

The intention of this series of experiments was to assess the feasibility of performing impedance-matching experiments on a microscopic scale. Figure 10 is an example of a target design for such an experiment, in this case intended to measure the shock velocities in aluminum and platinum and to provide a point on the platinum Hugoniot assuming knowledge of the aluminum equation of state. The two steps in the aluminum are to ensure that the shock velocity is constant, i.e., the shock is flat-topped in pressure and not decaying. We plan to eventually use molybdenum as the substrate-standard material. We are in the process of obtaining high-pressure EOS data on molybdenum in nuclear tests and expect to use it as a standard for all high-pressure, impedance-matching experiments.

So far we have demonstrated that we can use the step technique to measure shock velocities, but we do not believe we have sufficient resolution to measure more than one step. To obtain the necessary resolution we will need either a higher energy laser or a more sensitive, broader range streak

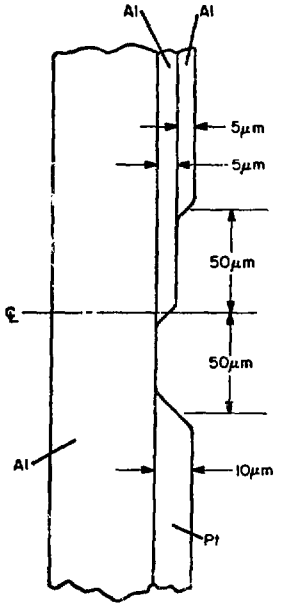

Fig. 10. Proposed target design for laser EOS measurements. A laser beam 200 to 400 μm in diameter impinges along the center line. Shock emergence is observed at various depths in aluminum and platinum to determine the relative shock velocities in the two materials.

camera. With a higher energy laser we can make the spot size larger and thereby spread the steps farther apart than the 50 μm indicated in Fig. 10, making them easier to resolve on the photocathode. With a more sensitive streak camera, we could simply increase magnification.

Perhaps the most significant demonstration of the present studies is the fact that shock widths are in the submicrometer range at pressures of a few megabars.

In the near future we hope to determine the reason for apparent shock decay. To do a meaningful impedance-matching experiment we must have a flat-topped shock persist during penetration of all the layers across which we measure time intervals. One way to obtain a cleaner, flatter pressure pulse is to construct a microscopic flyer plate. The plate would be accelerated by blowoff from the laser and then would strike the test plate, on the back of which we would have the layers for impedance matching. This technique also would eliminate the hot-electron problem since the electrons could not leave the flyer plate because of the resulting charge separation. It does not prevent fast ions accelerated by the electrons from leaving, however, but the ions cannot penetrate the test plate as deeply and therefore preheating is much less at the back surface.

Because the dynamic range of fast streak cameras is so limited, we have been seeking techniques for observing shock breakthrough and free-surface motion that do not depend on the shock's own radiation. This way we avoid the very critical T^4 dependence of intensity. One such technique is to shine a second laser off the back surface and observe the change in reflectivity of the metal when it is shocked. This has the advantage that the reflected light will be relatively constant from shot to shot, but may not give time resolution as good as we obtain in direct observation of the shock breakthrough.

ACKNOWLEDGMENTS

The authors would like to thank Dean Sutphin for his help in setting up the streak cameras and tutoring us in their operation. We also thank A. Campillo, A. Ellis, A. Engelhart, D. Giovanielli, M. Henderson, I. Johnson, G. McCall, C. Ragan, R. Robertson, E. Robinson, S. Shapiro, and E. Shunk for their help in carrying out the experiment; the members of the laser target fabrication group for making and mounting our aluminum targets; and the Laser Fusion Program members for their cooperation and support.

REFERENCES

1. C. G. M. van Kessel and R. Sigel, "Observation of Laser-Driven Shock Waves in Solid Hydrogen," Phys. Rev. Lett. 33, 1020-1023 (1974).
2. C. B. M. van Kessel, "Shock Compression of Plane Targets by Laser Ablation," Z. Naturforsch. 30a, 1581-1593 (1975).
3. D. Billon, D. Cognard, J. Launspach, C. Patou, D. Redon, and D. Schirmann, "Experimental Study of Plane and Cylindrical Laser Driven, Shock Wave Propagation," Optics Communications 15, 108-111 (1975).
4. C. E. Ragan III, "Design Considerations for a High-Pressure, Equation-of-State Experiment," Los Alamos Scientific Laboratory report LA-5615-MS (1974).
5. C. E. Ragan III, M. G. Silbert, and B. C. Diven, "Shock Compression of Molybdenum to 2.0 TPa by Means of a Nuclear Explosion," J. Appl. Phys. 48, 2860-2870 (1977).
6. D. V. Giovanielli, 'Wavelength Effects in Laser Fusion," Bull. Am. Phys. Soc. 21, 1047 (1976).
7. D. W. Forslund, J. M. Kindell, K. Lee, and E. L. Lindman, "Absorption of Laser Light on Self-Consistent Plasma Density Profiles," Phys. Rev. Lett. 36, 35-38 (1976).
8. D. W. Forslund, J. M. Kindell, and K. Lee, "Theory of Hot-Electron Spectra at High Laser Intensity, Phys. Rev. Lett. 39, 284-288 (1977).
9. D. H. Gill, R. C. Hyer, P. N. Mace, G. H. McCall, J. McLeod, J. E. Perry, Jr., and B. E. Watt, "Large Nd:Glass Laser System for Plasma Production," Bull. Am. Phys. Soc. 17, 1052 (1972).
10. D. H. Gill, R. C. Hyer, P. N. Mace, J. McLeod, J. E. Perry, C. H. Reed, R. H. Robertson, N. J. Terrell, and B. E. Watt, "A High-Power Nd: Glass Laser System for Fusion Research," IEEE J. Quantum Electronics, Vol. QE-10, 688-689 (1974).
11. D. J. Bradley, "Methods of Generation, Ultrashort Light Pulses: Picosecond Techniques and Applications, Ch. 2, pp. 17-81, Topics in Applied Physics, Vol. 18, ed. S. L. Shapiro (Springer Verlag, Berlin, 1977).
12. Ya. B. Zel'dovich and Yu. P. Raizer, Physics of Shock Waves and High-Temperature Hydrodynamic Phenomena, Vol. 2, pp. 773-777 (Academic Press, New York and London, 1966).
13. L. V. Al'tshuler, S. B. Kormer, M. I. Brazhnik, L. A. Vladimirov, M. P. Speranskaya, and A. I. Funtikov, "Isentropic Compressibility of Aluminum, Copper, Lead, and Iron at High Pressures," Sov. Phys.-JETP 11, 766-775 (1960).